Interaction of gold nanosurfaces/nanoparticles with collagen-like peptides

Ming Tang[a], Neha S. Gandhi[b], Kevin Burrage[b,c], and YuanTong Gu[a]*

[a] *School of Chemistry Physics and Mechanical Engineering, Queensland University of Technology, Brisbane, Australia*

[b] *School of Mathematical Sciences and* [c]*ARC Centre of Excellence for Mathematical and Statistical Frontiers, Queensland University of Technology – Brisbane 4001 – Australia*

Ming Tang: m21.tang@hdr.qut.edu.au

Corresponding author: yuantong.gu@qut.edu.au

Abstract

Nanotechnology has quickly emerged as a promising research field with potential effects in disease treatments. For example, gold nanoparticles (AuNPs) have been extensively used in diagnostics and therapeutics. When administrated into human tissues, AuNPs first encounter extracellular matrix (ECM) molecules. Amongst all the ECM components, collagen is the main tension-resisting constituent, whose biofunctional and mechanical properties are strongly dependent on its hierarchical structure. Therefore, an in-depth understanding of the structural response of collagen to the presence of gold nanosurfaces (AuNS) and AuNPs is crucial in terms of clinical applications of AuNPs. However, detailed understanding of the molecular-level and atomic-level interaction between AuNS/AuNPs and collagen in the ECM is elusive. In this study, comprehensive molecular dynamics (MD) simulations have been performed to investigate the molecular behaviour of a collagen molecule segment (CMS) in the presence of AuNS/AuNPs in explicit water, aiming to explore the interaction of AuNS/AuNPs with collagen triple helices at the molecular and atomic levels. The results show that the CMS form a rapid association with AuNS/AuNPs and undergoes a severe unfolding upon adsorption on AuNS/AuNPs, indicating an unfolding propensity of gold surfaces. We conclude that collagen triple helices unfold readily on AuNS and bare AuNPs, due to the interaction of gold surfaces with the protein backbone. The revealed clear unfolding nature and the unravelled atomic-level unfolding mechanism of collagen triple helices onto AuNPs contribute to the development of AuNPs for biomedical and therapeutic applications, and the design of gold-binding proteins.

Keywords: Collagen; Gold nanoparticles; Gold nanosurfaces; Protein adsorption; Unfolding; Molecular dynamics simulation; Collagen molecules

1 Instruction

Protein-inorganic surface interactions have been extensively used in nanobiotechnology for diagnostic and therapeutic applications (1). In this framework, protein-gold interactions have been widely investigated for biomedical applications (2), due to its ease of synthesis, functionalization and shape control (3), biocompatibility (4) and tunable optical properties. The potential clinical applications include antibiotics (5), wounds treatment (6), drug-delivery (7, 8), biomedicine (9), and various other advanced clinical diagnostic and therapeutic nanotechnologies (10). This sparks the urgent need for a thorough understanding of how gold nanoclusters adjust their properties in biological media (plasma, cell membranes and various intracellular environments), as well as how the biological milieu constituents (water, proteins, proteoglycans, lipids and DNA) respond to the presence of gold nanoclusters.

Despite the great significance of protein-gold interactions, understanding of the underlying physio-chemical principles remains in its infancy. To date, detailed structural and dynamical characterization of biomolecular interactions with surfaces via experimental studies is not feasible due to technical limitations (11). Alternatively, computational methods such as density functional theory (DFT) calculations, coarse-grained Monte Carlo simulations, and MD simulations have been widely employed to elucidate the atomistic foundations of protein-AuNS interactions (2). Amongst these computational approaches, atomistic MD simulations, with the best compromise between accuracy and computational feasibility, represent the dominant tool for describing the interaction between AuNS and amino acids (12-15), peptides (16-29) and proteins (30-34). Specifically, the preferred orientations of all twenty amino acids on the Au (1 1 1) surface were investigated by Hoefling et al. (13). This study demonstrated that all amino acids prefer to interact with the Au (1 1 1) surface at least partially via their backbone, indicating an unfolding propensity of the gold surface. In addition, the presence of AuNS was found to be able to induce conformational changes of peptides (16, 19-21, 23, 27).

In contrast to the extensive investigations on the interaction of planar AuNS with amino acids and peptides, very few studies have been conducted to explore the interaction of AuNPs with amino acids and peptides, i.e., considering the AuNS with a radius of curvature. Particularly, MD simulations were performed to study the shape effect of gold surfaces on the adsorption of small peptides (23). The peptides presented weaker adsorption onto the surface of a AuNP with a diameter of 2 nm than onto the extended Au(1 1 1) surface, and the adsorption energy

increases (become less below zero) as the diameter of the AuNP becomes smaller (23). In addition, well-tempered metadynamics simulations were used to investigate the binding preferences of all standard amino acids except Pro to AuNPs with different diameters, and whether these binding preferences are governed by the backbone, the side chain or both (35). This study demonstrated that the binding strength of an amino acid is strongly dependent on its physical and chemical nature and the radius of curvature of the gold surface. Interestingly, amino acids with relatively complex side chain structure showed multiple binding configurations onto AuNPs (35).

Despite such great effort put forth on characterizing the interplay of AuNS/AuNPs with amino acids and peptides, very limited studies have been undertaken to explore the interaction of AuNS/AuNPs with proteins. More specifically, Hoefling et al. studied the interaction occurring between AuNS and two domains with high β-sheet content of the extracellular matrix (ECM) protein fibronectin (32). This study found that the domain-domain orientation altered but the protein did not unfold on AuNS within the simulation time, despite the strong interaction with AuNS. Moreover, to elucidate the physio-chemical basis of ubiquitin-AuNPs interactions, Brancolini and co-workers performed computational simulations on ubiquitin-AuNS complex at multiple levels (30). This work reported a minor unfolding of the 3_{10} helix of ubiquitin arising from the interaction with AuNS. Similarly, partial unfolding of the α-helix bundle was observed for fibrinogen, due to the interaction with AuNPs (36). In addition, Cohavi et al. investigated interactions of AuNPs with BLIP and BLIP fused with various natural amino acid homo-tripeptides via surface plasmon resonance (37). This work suggested an unfolding tendency of proteins on bare AuNPs, which may result in the corresponding loss of biological activities of proteins. Above all, the presence of AuNS/AuNPs can induce the conformational changes (such as unfolding and induced-fit) of peptides and proteins. Moreover, the binding strength of amino acids and biomolecules are strongly dependent on the curvature of gold surfaces, i.e., the diameter of AuNPs (23, 35, 36). Finally, amino acids (13), peptides (20, 28), and proteins (32, 33) preferably showed flat configuration on the gold surface.

In particular, understanding the interaction occurring between AuNS/AuNPs and ECM constituents is important for nanotechnological and clinical applications. On one hand, AuNPs have been extensively employed in biomedical and therapeutic applications. On the other hand, ECM proteins are the first biomolecules encountered by AuNPs when entering

into human tissues (38, 39). Amongst all the ECM components, collagen is the most common protein that has been extensively studied for tissue engineering (40-43) and cancer treatment (44). Collagen is a hierarchical structure, with the bottom level being a collagen molecule triple helix. Amongst all the types of collagens, type I collagen represents the most common one and attracts most interests among researchers. Type I collagen molecule consists of three polypeptides (two α_1 chains and one α_2 chain), where glycine occupying every third position of the amino acid sequence is a prerequisite for the formation of the triple-helical structure.

Despite the great importance of collagen-AuNS/AuNPs interactions, rare literatures focused on the interaction of collagen with AuNS/AuNPs at the molecular and atomic levels. Particularly, MD simulations were conducted to investigate the adsorption of collagen-like peptides onto AuNS, where slight partial unfolding was observed for the collagen molecule segments of natural type I and type III collagen molecules (31). However, the underlying structural and mechanistic details regarding the interaction of collagen with AuNS and bare AuNPs at the molecular and atomic levels remain unknown. Motivated by this knowledge gap, this study investigates the molecular behaviour of a collagen molecule segment (CMS) under the presence of AuNS or bare AuNPs with different diameters, aiming to explore the interaction of collagen molecule triple helices with AuNS and bare AuNPs at the molecular and atomic levels. The large size of the intact collagen molecule (~ 300 nm) together with the limit of computer power render simulating adsorption of an intact collagen molecule onto AuNS and AuNPs unachievable. Therefore, this study investigates the interaction of a human type I CMS with AuNS and AuNPs in explicit water using MD simulations. Our results demonstrate that the CMS forms a rapid association and strong interactions with AuNS and AuNPs, resulting in a severe unfolding of its triple-helical structure. The atomic-level unfolding mechanisms of collagen triple helices on gold surfaces are unveiled.

2 Computational models and methodology

2.1 Model building

The CMS was generated using the Triple Helical collagen Building Script (THeBuScr) (45) by inputting the following sequences (numbers correspond to residue numbers of the first and last amino acids in the sequences): $_{2,66}$GARGLPGTAGLPGM**K**GHRGFSGLDGAKGDA$_{31,95}$ (for chain A and chain C, respectively), and $_{34}$GARGFPGTPGLPGF**K**GIRGHNGLDGLKGQP$_{63}$ (for chain B). These sequences are parts

of the whole sequences of human type I collagen (PubMed entry number NP_000079 for α1 chains, and NP_000080 for α2 chain). To avoid artefacts from charged ends, we capped the N-termini and C-termini of each chain with Ace and Nme residues, respectively. Hence, each collagen polypeptide consists of ten Gly-X-Y triplets and two terminal residues (chain A, B, and C contain residues 1-32, 33-64, and 65-96, respectively), resulting in a CMS with a length of approximately 92 Å. Adsorption of collagen-like peptides with comparable length have been investigated in previous MD simulation studies (31, 46, 47). The sixteenth residues (denoted in bold in the sequences) along each chain were modified from Lys to hydroxylysine (Hyl), which is essential for the fibril formation (48).

The face-centred cubic [1 1 1] gold surface structure with a dimension of 137 Å × 139 Å × 12 Å (six-atoms thick) was used, enabling the full range of interactions with adsorbed atoms of the biomolecule. This structure was built using gmx nbox command in GROMACS 5.0.4 (49) based on the Au (1 1 1) unit cell available in INTERFACE_FF_1_5 (https://bionanostructures.com/interface-md/). The atomistic bare gold spherical nanoparticles with a diameter of 3 nm and 8 nm were generated using the Nanoparticle Builder Module of OpenMD (50). The positions of the gold atoms are determined based on the diameter of the AuNP using the gold lattice constant of 0.408 nm. The surface of the built AuNPs are not uniform and contains Au(1 1 1), Au(1 1 0) and Au(1 0 0) facets and edges. The area of the facets and edges is related to the shape and diameter of the AuNP.

2.2 Molecular dynamics simulation protocol

To investigate the molecular behaviour of the CMS in the presence of AuNS, MD simulations regarding the CMS adsorption onto AuNS (denoted as Sys. 1) were carried out. For comparison, the CMS in the absence of AuNS and AuNPs (denoted as Sys. 2) was equilibrated in explicit water without any restraint on the protein via MD simulations. To explore the interaction between the CMS and AuNPs with different diameters, MD simulations were performed on the adsorption of the CMS onto two bare AuNPs with a diameter of 3 nm (denoted as Sys. 3) and 8 nm (denoted as Sys. 4), respectively. Detailed information of the four systems regarding the water box type and dimension, number of counter ions, gold atoms and water molecules are provided in Table 1. In each system, the solutes (i.e., the CMS and AuNS/AuNP) were fully solvated with explicit TIP3P water molecules (51), making sure that there exists at least a 10 Å water boundary on all sides. Seven Cl^- were added as counter ions to neutralize the systems using tleap in AmberTools 16

(52). In Sys. 1, the initial minimum distance between the CMS and AuNS is 12.5 Å, rendering the protein outside the cutoff range (within 10 Å) of the protein-AuNS dispersion interaction. In Sys. 3 and Sys. 4, the initial minimum distance between the protein and AuNP is 6 Å, as the system is computationally expensive and we are more interested in the interaction of the CMS with AuNPs after adsorbing onto AuNPs. To explore the interaction between the CMS and AuNS, totally 8 MD simulations were carried out for Sys. 1, where each simulation started from an identical CMS-AuNS complex conformation, without setting initial atomic velocities for the system. To probe the interaction of the CMS with AuNPs, we performed 8 simulations for Sys. 3 and 16 simulations for Sys. 4. The simulations for Sys. 3 started from the same CMS-AuNP complex conformation, whereas the simulations for Sys. 4 started from two different CMS-AuNP complex conformations (eight simulations for each complex conformation). All MD simulations in this study were performed using the CUDA version of AMBER 16 biomolecular simulation package (53, 54) and the protein.ff14SB force field parameter sets (55). The parameters for Hyl were taken from the work of Varma et al. (56). The interactions between AuNS/AuNPs and the solution phase were modelled using the INTERFACE force field developed by Heinz et al. (57). In this force field, the Lennard-Jones potential parameters for gold atoms are: the equilibrium nonbonded distance r_0 = 2.951 Å and the equilibrium nonbonded energy ε_0 = 5.29 kcal/mol (58). To eliminate bad contacts within the models, each system underwent two rounds of energy minimizations. In the first round, the solutes were restrained with a harmonic potential of 50 kcal/mol·Å, whereas the solvent was free to relax for 2000 steps, consisting of 1500 steepest decent steps before switching to the conjugate gradient method. In the second round, the complete systems were minimized with the same number of steepest decent and conjugate gradient steps, where both the protein and solvent were free to relax. Then, the minimized systems were heated for 125 ps from 0 K to 310K, where the CMS were held fixed with a positional restraint of 50 kcal/mol·Å. Further, the heated systems were equilibrated in an NPT ensemble for 500 ps at a constant pressure of one atmosphere with the Berendsen barostat (59), where no restraint was imposed on the protein. Finally, a production run was performed, where the temperature was fixed at 310 K using the Langevin thermostat with gamma_ln set to 2 (60) and the pressure was kept at one atmosphere with the Berendsen barostat (59) and a pressure coupling constant of 1 ps. In this study, AuNS and AuNPs were assumed rigid, hence were held fixed throughout the entire simulations for Sys. 1, Sys. 3 and Sys. 4. Bond lengths involving hydrogen atoms were restrained via SHAKE algorithm (61), thus allowing an integration

time step of 2 fs for solving the equations of motion. Long-range electrostatic interactions were computed via the particle mesh Ewald (PME) summation method, whereas non-bonded interactions were calculated with a cutoff distance of 1.0 nm. Periodic boundary conditions were employed in all dimensions. Coordinates of atoms were saved for every 2 ps for further analysis. To probe the interaction of AuNS with the CMS at the molecular and atomic levels, the production runs of the eight simulations for Sys. 1 were performed for 220 ns. For comparison, the production run of Sys. 2 with the CMS in the absence of AuNS and AuNPs was carried out for 220 ns as well. The simulations for Sys. 3 and Sys. 4 were carried out until the CMS unfolded severely on the AuNP.

Post data processing and analysis were performed using MATLAB 2016a (62), GROMACS 5.0.4 (49) and cpptraj in AmberTools 16 (52). UCSF Chimera 1.11.2 (http://www.cgl.ucsf.edu/chimera) (63) was used for visualization and GNUPLOT 4.6 (http://www.gnuplot.info) for plotting.

3 Results

This study probes the molecular behaviour of a human type I CMS in the presence of AuNS or AuNPs with different diameters, by performing comprehensive MD simulations on the CMS-AuNS/AuNP complex. This aims to explore the detailed interaction of AuNS/AuNPs with collagen triple helices at the molecular and atomic levels.

3.1 Interaction of the CMS with AuNS

3.1.1 Adsorption and unfolding configurations of the CMS on AuNS

Interestingly, the CMS in all eight simulations for Sys. 1 formed a rapid association with AuNS and underwent severe unfolding on the surface, indicating an unfolding propensity of AuNS. The consistent rapid association of the peptide with AuNS comes from the charged layers above the AuNS, which is induced by the orientational ordering of the water molecules therein (29). Fig. 1(A) displays the final snapshot of an exemplar trajectory, wherein the CMS unfolded severely on AuNS, and the adsorbed peptides showed a flat conformation on the gold surface. The unfolding behaviour and the flat conformation is due to the fact that all types of amino acids prefer to interact with AuNS at least partially via their backbone, thus maximizing the contact area (13). Since the adsorption pattern onto AuNS of an amino acid in biomolecules is intimately related to its chemical environment (such as neighbouring

residues), here we did not compare the adsorbed conformations of all types of amino acids with those in publications. Given that Gly occupies every third position of the amino acid sequence along the three collagen molecule polypeptides, it is important to understand its adsorbed conformation on AuNS. Fig. 1(B) shows the front view of the chain C region (coloured in green in Fig. 1(A)) containing residues with a residue number ranging from 84 to 96, where the backbone is displayed with ribbon style and all atoms are hidden except those of Gly residues. As demonstrated in Fig. 1(B), the conformation of Gly residues on AuNS is consistent with that reported in (13): i) the backbone prefers a flat conformation; ii) the NH-moiety is marginally pointing upwards the gold surface, whereas the carbonyl oxygen is pointing towards. We note that the nearly flat configuration of the backbone of the entire chain region displayed in Fig. 1(B) might arise from the high content of Gly.

3.1.2 Radial distribution functions for interactions between the CMS and AuNS

A closer look at configurations of the CMS-AuNS complex in all of the simulations for Sys. 1 suggests that AuNS form direct interactions with the CMS backbone adsorbed on AuNS rather than through water shells. To explore the atomic-level interaction of the CMS with AuNS, we examined radial distribution functions (RDFs) for the main chain atoms (i.e., H, O, N, C, CA) of the CMS to AuNS, which describe distributions of the main chain atoms around the AuNS. Fig. 2 displays the RDFs for the main chain atoms of the CMS ((A)) and all of the Gly residues ((B)) around the AuNS. As can be seen from Fig. 2(A), there is a clear peak for the RDF of each main chain atom, suggesting their interactions with the gold surface. The first peak of RDFs for all of the main chain atoms (Fig. 2(A)) at a distance of less than 3.5 Å indicates that the CMS main chain atoms interact directly with AuNS rather than through water shells. This agrees with the results reported in the literature that AuNS prefers to interact with amino acids directly (28). Further, as illustrated in Fig. 2(B), the first peaks of RDFs for the main chain atoms of Gly residues occur at a distance with a relationship of r(O) < r(C) < r(CA) < r(N) < r(H), which further confirms the adsorbed conformation of Gly residues on AuNS displayed in Fig. 1(B). In addition, the peaks of RDFs for the carbonyl oxygen in Fig. 2(A) and Fig. 2(B) are sharper and higher than those of other main chain atoms. This reveals that AuNS forms stronger interaction with the carbonyl oxygen of the adsorbed protein than other main chain atoms. In sum, AuNS directly interact with the CMS main chain atoms, which confines them forming inter-chain hydrogen bonds with neighbouring chains, thus resulting in a significant unfolding of the triple-helical structure of

the CMS. In contrast to unfolding in the presence of AuNS, visualization of the trajectory from the simulation of Sys. 2 shows that the CMS preserved its secondary structure in the absence of AuNS throughout the simulation time.

3.2 Interaction of the CMS with AuNPs

AuNPs have been extensively used for diagnostics and therapeutics, such as biosensing, cancer treatment and drug delivery. Upon entering into human tissues, AuNPs first come across ECM biomolecules (38, 39). Among all the components of ECM, collagen is the most common protein. The biofunctional and mechanical properties of collagen are determined by its structure at different levels of hierarchies. Therefore, an in-depth understanding of the structural response of collagen (with a persistence length of ~14 nm) to the presence of gold clusters is of great importance.

In the previous section, the interaction of collagen triple helices with AuNS was investigated. However, peptides interact less strongly with the Au(1 0 0) surface than with the Au(1 1 1) surface (14, 16). In addition, surfaces with a radius of curvature smaller than the persistence length of the chain biomolecule are less attractive than planar surfaces (23). Therefore, it is crucial to investigate the structural response of collagen to the presence of AuNPs, as AuNPs comprise Au(1 1 1), Au(1 1 0), and Au(1 0 0) facets and edges. This section presents detailed interactions between the CMS and bare AuNPs with two different diameters, namely 3 nm and 8 nm, at the molecular and atomic levels.

3.2.1 Adsorption and unfolding configurations of the CMS on AuNPs

In all of the simulations on the CMS interacting with AuNPs (Sys. 3 and Sys. 4), the CMS rapidly formed a CMS-AuNP complex with the AuNP, but the initiation time and the configurations of the complex are different among different simulations starting from an identical complex conformation for the same system. The difference in the configurations of the complex demonstrates that the CMS was initially in the diffusion sate, as the initial distance between the CMS and the AuNPs is over 6 Å. The random contact patterns together with the rapid formation of the CMS-AuNP complex indicate the rather unspecific binding of the CMS to AuNPs. Fig. 3 displays the front view ((A)) and top view ((B)) of a representative snapshot of the CMS-AuNP complex extracted from one of the simulations for Sys. 3, where the CMS is unfolded on the AuNP with a diameter of 3 nm. Fig. 4 shows the top view ((A)) and front view ((B)) of a representative snapshot of the CMS-AuNP complex extracted from

one of the simulations for Sys. 4, where the CMS is unfolded on the AuNP with a diameter of 8 nm. Interestingly, the CMS in all of the 16 simulations for Sys. 4 fully adsorbed on the AuNP with a diameter of 8 nm, whereas the CMS in all the simulations for Sys. 3 only partially adsorbed on the AuNP with a diameter of 3 nm. This is because when the radius of curvature is smaller than the persistence length of the molecule, surfaces with a larger radius of curvature are more attractive to the molecule than surfaces with a smaller radius of curvature (23). However, the CMS or the portion of the CMS adsorbed on the AuNPs unfolded severely on different facets and ages of the AuNPs with both diameters, indicating the unfolding propensity of AuNPs. As illustrated in Fig. 3 and Fig. 4, the CMS prefers an extended configuration upon adsorption onto different facets of AuNPs with different diameters. Similar extended conformations were previously reported for different small peptides on a gold surface with a radius of curvature of 2 nm (23). However, as illustrated in Fig. 1, Fig. 3 and Fig. 4, the unfolding patterns of the protein on AuNS and AuNPs differ from each other, due to the difference in their radius of curvature and that AuNPs consist of multiple facets.

3.2.2 Radial distribution functions for interactions between the CMS and AuNPs

A closer look at configurations of the CMS-AuNP complex in all of the simulations for Sys. 3 and Sys.4 suggests that AuNPs interact directly with the CMS or the CMS portion adsorbed on the AuNP rather than via a solvation shell. To further explore detailed interactions of the CMS with AuNPs, we examined the RDFs for the main chain atoms of the CMS to AuNPs. Fig. 5 displays the RDFs for the main chain atoms around the AuNP with a diameter of 3 nm (Fig. 5(A)) and 8 nm (Fig. 5(B)). AuNPs directly interacting with the adsorbed CMS or CMS portion is reflected by the fact that the first peaks of RDFs in Fig. 5(A) and Fig. 5(B) for all of the main chain atoms occur at a distance of less than 3.5 Å. This is consistent with the results reported in the literature that standard amino acids interact with AuNPs with different diameters via their backbone rather than though a solvation shell (35). Moreover, the peaks of RDFs for the amide nitrogen (N), carbonyl oxygen (O) and amide hydrogen (H) in both Fig. 5(A) and Fig. 5(B) reflect their interactions with the AuNPs. This is justified by the fact that the anchoring bonding interactions of N-Au and O-Au, as well as the nonconventional N-H⋯Au hydrogen bonding interactions modulate the interaction between amino acids and gold surfaces (64). In addition, among the five main chain atoms, AuNPs preferably interact with the carbonyl oxygen, which is demonstrated by the sharper and higher peaks of the

RDFs for the carbonyl oxygen in both Fig. 5(A) and Fig. 5(B) than those for other main chain atoms.

3.3 Unfolding mechanism of the CMS on AuNS and AuNPs

It is important to explore the unfolding mechanism of the CMS on AuNS and AuNPs with different diameters. Interestingly, we found that Gly residues in chain regions with a relatively flat backbone configuration on the Au(1 1 1) facet of AuNPs adopt similar configurations as those on the planar Au(1 1 1) surface as displayed in Fig. 1(B). For instance, the backbone of Gly_17 adopts a nearly flat conformation on the Au(1 1 1) facet of the AuNP with a diameter of 8 nm, where the carbonyl oxygen is pointing towards the gold surface, whereas the NH-moiety is slightly pointing upwards (Fig. 4(C)). The slightly inclined backbone conformation of Gly_17 comes from the incompletely flat backbone conformation of the chain region, due to the curvature of the gold surface. In contrast, this uniform conformation was not always observed for Gly residues on other facets and edges of AuNPs with both diameters, due to different potentials around different facets coming from the difference in the structure.

The triple-helical structure of the CMS is stabilized by the conventional inter-chain hydrogen bonds formed between the amide hydrogen atom of a glycine in one peptide (chain id: i) and the carbonyl oxygen atom of a residue occupying the X position of the Gly_X_Y triplet in another peptide (chain id: i+1 or i-2). The presence of these inter-chain hydrogen bonds is under the condition that both the amide hydrogen of Gly in chain i and the carbonyl oxygen of the X residue in chain i+1 or i-2 point towards each other, i.e., point to the axis of the triple helix. For example, the amide hydrogen of Gly_20 in chain A forms a hydrogen bond with the carbonyl oxygen of Ile_50 in chain B (green dashed line in Fig. 4(C)). However, Gly residues adopt the configurations on the Au(1 1 1) facets that the NH-moieties only slightly point upwards the gold surfaces (e.g., Gly_17 displayed in Fig. 4(C) and the Gly residues showed in Fig. 1(B)), rendering them not capable of forming inter-chain hydrogen bonds with the X residues in neighbouring chains. In addition, AuNS and AuNPs favour the interactions with the carbonyl oxygen atoms of the protein backbone (as reflected by the carbonyl oxygen atoms in Fig. 4(C) and the RDFs in Fig. 2 and Fig. 5). This forces the carbonyl oxgens of the X residues pointing towards the gold surfaes, and hence prevents them from forming inter-chain hydrogen bonding interactions with the amide hydrogen of Gly in a neighbouring chain. These two factors together confine the formaion of the inter-chain hydrogen bonds in

collagen triple helices, thus leading to the severe unfolding of the collagen triple helices on AuNS and AuNPs.

4 Discussion

As already illustrated in Introduction, experimental approaches have significant limitations (11), rendering it infeasible to quantitatively validate the results demonstrated here. This study shows that collagen triple helices readily unfold on bare gold surfaces. Notably, slight partial unfolding was previously reported for collagen molecule segments on AuNS in the literature (31). However, the unfolding of collagen triple helices was attributed to the interaction of AuNS with protein side chains (e.g., OH and NH_3^+), which differs from the unfolding mechanism unveiled in the present study, where unfolding was demonstrated to originate from the interaction of AuNS/AuNPs with the backbone of collagen triple helices.

Moving beyond the very limited studies specifically concerned with collagen interacting with gold surfaces, there is strong support for the structure of the protein on gold surfaces presented here. Specifically, the observed unfolding behaviour of the CMS reflects the unfolding propensity reported for AuNS and bare AuNPs in previous studies (13, 30, 37). Furthermore, the obtained flat conformation of the CMS on AuNS is in good agreement with literatures, where amino acids (13), peptides (20, 28), and proteins (32, 33) presented to adopt flat configurations on gold surfaces. In addition, the extended configuration of the CMS on AuNPs and the direct interaction between AuNPs and the protein backbone are consistent with the results reported in the literature (23, 35).

It is important to address the potential force field used for the characterization of AuNS and AuNPs. Here, we used the INTERFACE force field (57), which was reported to yield the water layering structure adjacent to the metal surface consistent with experimental observations, and to reproduce the noncovalent adsorption of biomolecules obtained from experiments (16, 65). This force field has been extensively employed for the characterization of the interactions of AuNS/AuNPs with amino acids and biomolecules (15-17, 23, 29, 35, 66, 67). Unlike the GoIP force field (14, 68), the INTERFACE force field does not characterize the polarization of the gold surfaces (69), which is believed to occur in the presence of charges. However, the unfolding phenomenon of the collagen triple-helical structure is unlikely to be affected by the lack of consideration of the gold surface polarization. Specifically, amino acids and residues of biomolecules prefer to interact with gold surfaces

with polarization at least partially via their backbone (13), thus leading to flat configurations on gold surfaces of amino acids (13), peptides (20, 28), and proteins (32, 33). On the other hand, glycine, which occupies every third position of the sequence along each collagen peptide and provides the biomolecule with flexibility (16, 17), is a nonpolar uncharged residue, rendering its interaction with gold surfaces independent of the surface polarization. This is justified by the fact that the equilibrium conformation of Gly on AuNS (Fig. 1(B)) and Gly_17 on AuNP (Fig. 4(C)) obtained here are identical to that of Gly on the gold surface with polarization reported in the literature (13). When the protein backbone adsorbs onto AuNS/AuNPs, the NH-moiety of Gly residues only slightly points upwards the surface, and the carbonyl oxygen of residues occupying the X positions of the Gly_X_Y triplets is forced to point towards AuNS/AuNPs. This renders them no longer capable of hydrogen bonding to each other, thus inducing significant unfolding of the triple-helical structure. To date, this atomic-level unfolding mechanism has not been reported in the literature.

Even if the final adsorbed configuration and the unfolding extent may vary among different collagen triple-helical segments on AuNS/AuNPs, the observed unfolding phenomenon and the unraveled atomic-level unfolding mechanism occur to any types of collagen molecules, and the collagen-like domains of other proteins such as c1q and adiponectin. In addition, other glycine-rich proteins may also easily adsorb and unfold on AuNS and bare AuNPs, as glycine renders the proteins very flexible thus favouring their adsorption and unfolding onto the gold surfaces (27). Given that collagen molecules assemble into fibril rapidly in the ECM, local unfolding of the collagen and collagen-like proteins may occur under the presence of bare AuNPs.

It is crucial to understand the fate of bare AuNPs when entering into human tissues. Firstly, it is inevitable, at least under the conditions considered here, for proteins to adsorb onto bare AuNPs (29, 32). Notably, in the ECM, charged residues of proteins are surrounded by counter ions, which may result in the screening of the charged residues. However, it is still possible for collagen to form the collagen-AuNPs complex, and partially unfold on bare AuNPs. Firstly, hydrophobic residues with long side chains (e.g., Leu) can function as anchors of collagen to AuNPs during the initiation of the collagen-AuNPs complex (29). Further, type I collagen molecule contains only ~14% charged residues, thus allowing the partial contact of collagen with AuNPs with small radius of curvatures. In addition, glycine occupies every third position of the collagen molecule polypeptides, and collagen molecules

adsorbed on bare AuNPs can readily undergo partial unfolding as demonstrated in this study. Due to the unfolding propensity and instability of bare AuNPs, AuNPs used for biomedical applications are normally coated. However, relatively less is known about the fate of those AuNPs after they fulfill the desired missions. The present study emphasizes the potential health risk induced by the presence of bare AuNPs in the human body.

It is also important to know the structural response of collagen triple helices to the presence of other solid surfaces such as titanium and stainless steel. According to this work, collagen triple-helical structure may unfold on solid surfaces that prefer to interact at least partially with the protein backbone, thus destroying the inter-chain hydrogen bonds of the triple helices. Indeed, unfolding of collagen-like peptides was also previously reported on a titanium surface (46).

This study provides significant insights into the development of AuNPs for disease treatments, and the design of gold-binding proteins. It is demonstrated that collagen molecules and collagen-like peptides unfold easily on bare AuNPs. This suggests the potential health risks associated with AuNPs, thus emphasising the significance of testing the health risks of AuNPs for biomedical and therapeutic applications. In addition, based on the unfolding propensity of collagen molecules obtained here, it is essential, in order to extend collagen permanence onto gold-based surfaces, to link the collagen molecules covalently to the gold interfaces, thus enhancing the biocompatibility.

The present study has several limitations. On the one hand, all of the simulations for Sys. 1 and Sys. 3 were performed starting from an identical initial conformation of the CMS-AuNS complex, due to the large size of the model investigated, the limit of computer power, and the large number of simulations required for each starting conformation of the complex. Ideally, various complex conformations with different relative positions of the CMS to AuNS could be considered. For instance, three different relative positions could be explored, where each case corresponds to one of the three collagen peptides being closest to AuNS in terms of the N-terminal regions of the triple helix. However, the unfolding phenomenon reported here are not likely to be influenced by the identical initial conformation of the complex. On the other hand, the INTERFACE force field (57) used to describe the interactions of the biomolecule with AuNS and AuNPs does not consider the polarization effect of the surface, which is demonstrated to exist in the presence of charges (14, 68). Thus, the final configuration of the adsorbed CMS onto AuNS and AuNPs might be different with those obtained with the

potential of gold atoms being described by the GoIP force field (14, 68). However, the unfolding phenomenon is justified to not be influenced by the lack of characterization of the surface polarization and the exact final adsorbed configuration of the CMS-AuNS/AuNPs complex is not the focus of this study.

5 Conclusions

By interrogating the results of comprehensive MD simulations on the CMS-AuNS/AuNPs complex, we find that collagen molecule triple helices are able to form a rapid association with AuNS/AuNPs, indicating that no bare AuNPs exist in the ECM. In addition, collagen triple helices unfold readily on both planar AuNS and AuNPs with different diameters, due to the interaction between gold atoms and the protein backbone. The revealed unfolding nature and the unravelled atomic-level unfolding mechanism contributes to the development of AuNPs for biomedical and therapeutic applications, and the design of gold-binding proteins. In addition, the presented results provide insights into the development of collagen-AuNP composites, which might be used for biomedical, clinical and tissue engineering applications.

6 Conflicts of interest

The authors declare that they have no conflict of interest.

7 Acknowledgements

The authors thank Hendrik Heinz (Department of Chemical and Biological Engineering, University of Colorado at Boulder, Boulder, Colorado, USA) for his detailed explanations of the INTERFACE force field. This research was funded by ARC Discovery project (DP150100828). The High Performance Computing resources provided by Queensland University of Technology (QUT) are gratefully acknowledged. Also, the financial support of China Scholarship Council (CSC) scholarship from Chinese government and Top-up scholarship from QUT are greatly appreciated.

8 Reference

1. Ozboyaci M, Kokh DB, Corni S, Wade RC. Modeling and simulation of protein–surface interactions: achievements and challenges. Quarterly reviews of biophysics. 2016;49.
2. Charchar P, Christofferson AJ, Todorova N, Yarovsky I. Understanding and Designing the Gold–Bio Interface: Insights from Simulations. Small. 2016;12(18):2395-418.
3. Goswami N, Zheng K, Xie J. Bio-NCs–the marriage of ultrasmall metal nanoclusters with biomolecules. Nanoscale. 2014;6(22):13328-47.
4. Shukla R, Bansal V, Chaudhary M, Basu A, Bhonde RR, Sastry M. Biocompatibility of gold nanoparticles and their endocytotic fate inside the cellular compartment: a microscopic overview. Langmuir. 2005;21(23):10644-54.
5. Feng Y, Chen W, Jia Y, Tian Y, Zhao Y, Long F, et al. N-Heterocyclic molecule-capped gold nanoparticles as effective antibiotics against multi-drug resistant bacteria. Nanoscale. 2016;8(27):13223-7.
6. Li Y, Tian Y, Zheng W, Feng Y, Huang R, Shao J, et al. Composites of Bacterial Cellulose and Small Molecule‐Decorated Gold Nanoparticles for Treating Gram‐Negative Bacteria‐Infected Wounds. Small. 2017;13(27).
7. Lei Y, Tang L, Xie Y, Xianyu Y, Zhang L, Wang P, et al. Gold nanoclusters-assisted delivery of NGF siRNA for effective treatment of pancreatic cancer. Nature communications. 2017;8:15130.
8. Deyev S, Proshkina G, Ryabova A, Tavanti F, Menziani MC, Eidelshtein G, et al. Synthesis, Characterization, and Selective Delivery of DARPin–Gold Nanoparticle Conjugates to Cancer Cells. Bioconjugate chemistry. 2017;28(10):2569-74.
9. Dreaden EC, Alkilany AM, Huang X, Murphy CJ, El-Sayed MA. The golden age: gold nanoparticles for biomedicine. Chemical Society Reviews. 2012;41(7):2740-79.
10. Lim E-K, Kim T, Paik S, Haam S, Huh Y-M, Lee K. Nanomaterials for theranostics: recent advances and future challenges. Chemical reviews. 2014;115(1):327-94.
11. Cohavi O, Corni S, De Rienzo F, Di Felice R, Gottschalk KE, Hoefling M, et al. Protein–surface interactions: challenging experiments and computations. Journal of Molecular Recognition. 2010;23(3):259-62.
12. Hoefling M, Iori F, Corni S, Gottschalk K-E. Interaction of amino acids with the Au (111) surface: adsorption free energies from molecular dynamics simulations. Langmuir. 2010;26(11):8347-51.
13. Hoefling M, Iori F, Corni S, Gottschalk KE. The conformations of amino acids on a gold (111) surface. ChemPhysChem. 2010;11(8):1763-7.
14. Wright LB, Rodger PM, Corni S, Walsh TR. GolP-CHARMM: first-principles based force fields for the interaction of proteins with Au (111) and Au (100). Journal of chemical theory and computation. 2013;9(3):1616-30.
15. Feng J, Pandey RB, Berry RJ, Farmer BL, Naik RR, Heinz H. Adsorption mechanism of single amino acid and surfactant molecules to Au {111} surfaces in aqueous solution: design rules for metal-binding molecules. Soft Matter. 2011;7(5):2113-20.
16. Heinz H, Farmer BL, Pandey RB, Slocik JM, Patnaik SS, Pachter R, et al. Nature of molecular interactions of peptides with gold, palladium, and Pd− Au bimetal surfaces in aqueous solution. Journal of the American Chemical Society. 2009;131(28):9704-14.
17. Yu J, Becker ML, Carri GA. The influence of amino acid sequence and functionality on the binding process of peptides onto gold surfaces. Langmuir. 2011;28(2):1408-17.
18. Hughes ZE, Kochandra R, Walsh TR. Facet-Specific Adsorption of Tripeptides at Aqueous Au Interfaces: Open Questions in Reconciling Experiment and Simulation. Langmuir. 2017;33(15):3742-54.
19. Soltani N, Gholami MR. Increase in the β‐Sheet Character of an Amyloidogenic Peptide upon Adsorption onto Gold and Silver Surfaces. ChemPhysChem. 2017;18(5):526-36.

20. Bellucci L, Bussi G, Di Felice R, Corni S. Fibrillation-prone conformations of the amyloid-β-42 peptide at the gold/water interface. Nanoscale. 2017;9(6):2279-90.
21. Bellucci L, Corni S. Interaction with a gold surface reshapes the free energy landscape of alanine dipeptide. The Journal of Physical Chemistry C. 2014;118(21):11357-64.
22. Tang Z, Palafox-Hernandez JP, Law W-C, E. Hughes Z, Swihart MT, Prasad PN, et al. Biomolecular recognition principles for bionanocombinatorics: an integrated approach to elucidate enthalpic and entropic factors. ACS nano. 2013;7(11):9632-46.
23. Feng J, Slocik JM, Sarikaya M, Naik RR, Farmer BL, Heinz H. Influence of the shape of nanostructured metal surfaces on adsorption of single peptide molecules in aqueous solution. Small. 2012;8(7):1049-59.
24. Braun R, Sarikaya M, Schulten K. Genetically engineered gold-binding polypeptides: structure prediction and molecular dynamics. Journal of Biomaterials Science, Polymer Edition. 2002;13(7):747-57.
25. Verde AV, Acres JM, Maranas JK. Investigating the specificity of peptide adsorption on gold using molecular dynamics simulations. Biomacromolecules. 2009;10(8):2118-28.
26. Heinz H. Computational screening of biomolecular adsorption and self‐assembly on nanoscale surfaces. Journal of computational chemistry. 2010;31(7):1564-8.
27. Vila Verde A, Beltramo PJ, Maranas JK. Adsorption of homopolypeptides on gold investigated using atomistic molecular dynamics. Langmuir. 2011;27(10):5918-26.
28. Palafox-Hernandez JP, Tang Z, Hughes ZE, Li Y, Swihart MT, Prasad PN, et al. Comparative study of materials-binding peptide interactions with gold and silver surfaces and nanostructures: a thermodynamic basis for biological selectivity of inorganic materials. Chemistry of Materials. 2014;26(17):4960-9.
29. Penna MJ, Mijajlovic M, Biggs MJ. Molecular-level understanding of protein adsorption at the interface between water and a strongly interacting uncharged solid surface. Journal of the American Chemical Society. 2014;136(14):5323-31.
30. Brancolini G, Kokh DB, Calzolai L, Wade RC, Corni S. Docking of ubiquitin to gold nanoparticles. ACS nano. 2012;6(11):9863-78.
31. Gopalakrishnan R, Singam EA, Sundar JV, Subramanian V. Interaction of collagen like peptides with gold nanosurfaces: a molecular dynamics investigation. Physical Chemistry Chemical Physics. 2015;17(7):5172-86.
32. Hoefling M, Monti S, Corni S, Gottschalk KE. Interaction of β-sheet folds with a gold surface. PloS one. 2011;6(6):e20925.
33. Ozboyaci M, Kokh D, Wade R. Three steps to gold: mechanism of protein adsorption revealed by Brownian and molecular dynamics simulations. Physical Chemistry Chemical Physics. 2016;18(15):10191-200.
34. Brancolini G, Maschio MC, Cantarutti C, Corazza A, Fogolari F, Bellotti V, et al. Citrate stabilized gold nanoparticles interfere with amyloid fibril formation: D76N and ΔN6 β2-microglobulin variants. Nanoscale. 2018;10(10):4793-806.
35. Shao Q, Hall CK. Binding preferences of amino acids for gold nanoparticles: A molecular simulation study. Langmuir. 2016;32(31):7888-96.
36. Tavanti F, Pedone A, Menziani MC. Competitive binding of proteins to gold nanoparticles disclosed by molecular dynamics simulations. The Journal of Physical Chemistry C. 2015;119(38):22172-80.
37. Cohavi O, Reichmann D, Abramovich R, Tesler AB, Bellapadrona G, Kokh DB, et al. A Quantitative, Real‐Time Assessment of Binding of Peptides and Proteins to Gold Surfaces. Chemistry-A European Journal. 2011;17(4):1327-36.
38. Lacerda SHDP, Park JJ, Meuse C, Pristinski D, Becker ML, Karim A, et al. Interaction of gold nanoparticles with common human blood proteins. ACS nano. 2009;4(1):365-79.

39. Lundqvist M, Stigler J, Elia G, Lynch I, Cedervall T, Dawson KA. Nanoparticle size and surface properties determine the protein corona with possible implications for biological impacts. Proceedings of the National Academy of Sciences. 2008;105(38):14265-70.
40. Yang J, Yang X, Wang L, Zhang W, Yu W, Wang N, et al. Biomimetic nanofibers can construct effective tissue-engineered intervertebral discs for therapeutic implantation. Nanoscale. 2017;9(35):13095-103.
41. Tidu A, Ghoubay-Benallaoua D, Teulon C, Asnacios S, Grieve K, Portier F, et al. Highly concentrated collagen solutions leading to transparent scaffolds of controlled three-dimensional organizations for corneal epithelial cell colonization. Biomaterials science. 2018;6(6):1492-502.
42. Wang X, Coradin T, Hélary C. Modulating inflammation in a cutaneous chronic wound model by IL-10 released from collagen–silica nanocomposites via gene delivery. Biomaterials science. 2018;6(2):398-406.
43. Udhayakumar S, Shankar KG, Sowndarya S, Rose C. Novel fibrous collagen-based cream accelerates fibroblast growth for wound healing applications: in vitro and in vivo evaluation. Biomaterials science. 2017;5(9):1868-83.
44. Raeesi V, Chan WC. Improving nanoparticle diffusion through tumor collagen matrix by photo-thermal gold nanorods. Nanoscale. 2016;8(25):12524-30.
45. Rainey JK, Goh MC. An interactive triple-helical collagen builder. Bioinformatics. 2004;20(15):2458-9.
46. Monti S. Molecular dynamics simulations of collagen-like peptide adsorption on titanium-based material surfaces. The Journal of Physical Chemistry C. 2007;111(16):6086-94.
47. Gopalakrishnan R, Balamurugan K, Singam ERA, Sundaraman S, Subramanian V. Adsorption of collagen onto single walled carbon nanotubes: a molecular dynamics investigation. Physical Chemistry Chemical Physics. 2011;13(28):13046-57.
48. Morgan PH, Jacobs HG, Segrest JP, Cunningham LW. A Comparative Study of Glycopeptides Derived from Selected Vertebrate Collagens A POSSIBLE ROLE OF THE CARBOHYDRATE IN FIBRIL FORMATION. Journal of Biological Chemistry. 1970;245(19):5042-8.
49. Berendsen HJ, van der Spoel D, van Drunen R. GROMACS: A message-passing parallel molecular dynamics implementation. Computer Physics Communications. 1995;91(1):43-56.
50. Gezelter J, Kuang S, Marr J, Stocker K, Li C, Vardeman C, et al. OpenMD, an open source engine for molecular dynamics. University of Notre Dame: Notre Dame, IN; 2010.
51. Jorgensen WL, Chandrasekhar J, Madura JD, Impey RW, Klein ML. Comparison of simple potential functions for simulating liquid water. The Journal of chemical physics. 1983;79(2):926-35.
52. Duke R, Giese T, Gohlke H, Goetz A, Homeyer N, Izadi S, et al. AmberTools 16. University of California, San Francisco; 2016.
53. Case DA, Betz RM, Cerutti DS, T.E. Cheatham I, Darden TA, Duke RE, et al. AMBER 2016. University of University of California, San Francisco2016.
54. Salomon-Ferrer R, Götz AW, Poole D, Le Grand S, Walker RC. Routine microsecond molecular dynamics simulations with AMBER on GPUs. 2. Explicit solvent particle mesh Ewald. Journal of chemical theory and computation. 2013;9(9):3878-88.
55. Maier JA, Martinez C, Kasavajhala K, Wickstrom L, Hauser KE, Simmerling C. ff14SB: improving the accuracy of protein side chain and backbone parameters from ff99SB. Journal of chemical theory and computation. 2015;11(8):3696-713.
56. Varma S, Botlani M, Hammond JR, Scott HL, Orgel JP, Schieber JD. Effect of intrinsic and extrinsic factors on the simulated D‐band length of type I collagen. Proteins: Structure, Function, and Bioinformatics. 2015.
57. Heinz H, Lin T-J, Kishore Mishra R, Emami FS. Thermodynamically consistent force fields for the assembly of inorganic, organic, and biological nanostructures: the INTERFACE force field. Langmuir. 2013;29(6):1754-65.

58. Heinz H, Vaia R, Farmer B, Naik R. Accurate simulation of surfaces and interfaces of face-centered cubic metals using 12− 6 and 9− 6 Lennard-Jones potentials. The Journal of Physical Chemistry C. 2008;112(44):17281-90.
59. Berendsen HJ, Postma Jv, van Gunsteren WF, DiNola A, Haak J. Molecular dynamics with coupling to an external bath. The Journal of chemical physics. 1984;81(8):3684-90.
60. McQuarrie D. Statistical Mechanics Harper Collins. New York. 1976;19762.
61. Ryckaert J-P, Ciccotti G, Berendsen HJ. Numerical integration of the cartesian equations of motion of a system with constraints: molecular dynamics of n-alkanes. Journal of Computational Physics. 1977;23(3):327-41.
62. Quan BD. Molecular Control of Collagen Biomineralization in the Periodontium 2015.
63. Huang CC, Couch GS, Pettersen EF, Ferrin TE, editors. Chimera: an extensible molecular modeling application constructed using standard components. Pac Symp Biocomput; 1996: World Scientific.
64. Pakiari A, Jamshidi Z. Interaction of amino acids with gold and silver clusters. The Journal of Physical Chemistry A. 2007;111(20):4391-6.
65. Geada IL, Ramezani-Dakhel H, Jamil T, Sulpizi M, Heinz H. Insight into induced charges at metal surfaces and biointerfaces using a polarizable Lennard–Jones potential. Nature communications. 2018;9(1):716.
66. Heinz H, Jha KC, Luettmer-Strathmann J, Farmer BL, Naik RR. Polarization at metal–biomolecular interfaces in solution. Journal of The Royal Society Interface. 2010:rsif20100318.
67. Ferreira AF, Rai A, Ferreira L, Simões PN. Findings on the interaction of the antimicrobial peptide cecropin-melittin with a gold surface from molecular dynamics studies. European Biophysics Journal. 2017;46(3):247-56.
68. Iori F, Di Felice R, Molinari E, Corni S. GolP: An atomistic force‐field to describe the interaction of proteins with Au (111) surfaces in water. Journal of computational chemistry. 2009;30(9):1465-76.
69. Giesbers M, Kleijn JM, Stuart MAC. The electrical double layer on gold probed by electrokinetic and surface force measurements. Journal of colloid and interface science. 2002;248(1):88-95.

9 List of figures and tables

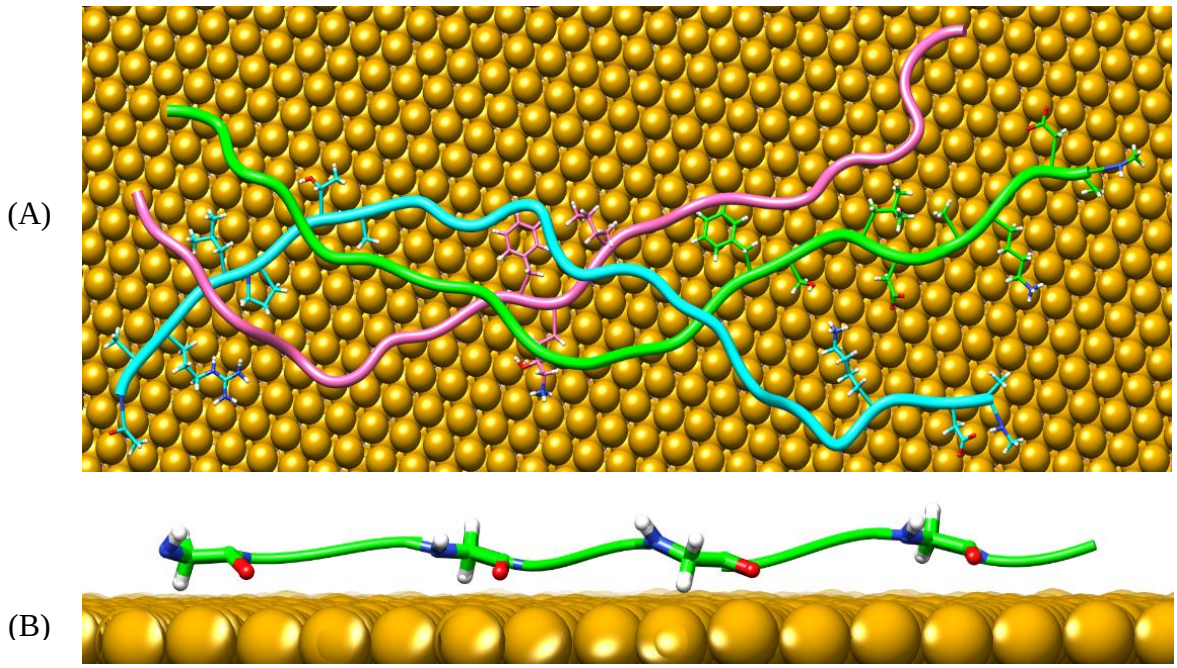

Fig. 1 An exemplar trajectory of the MD simulations on the CMS-AuNS complex: (A) final snapshot of the complex in this simulation; (B) zoomed in view of the conformation of a region in chain C (colored in green in (A)).

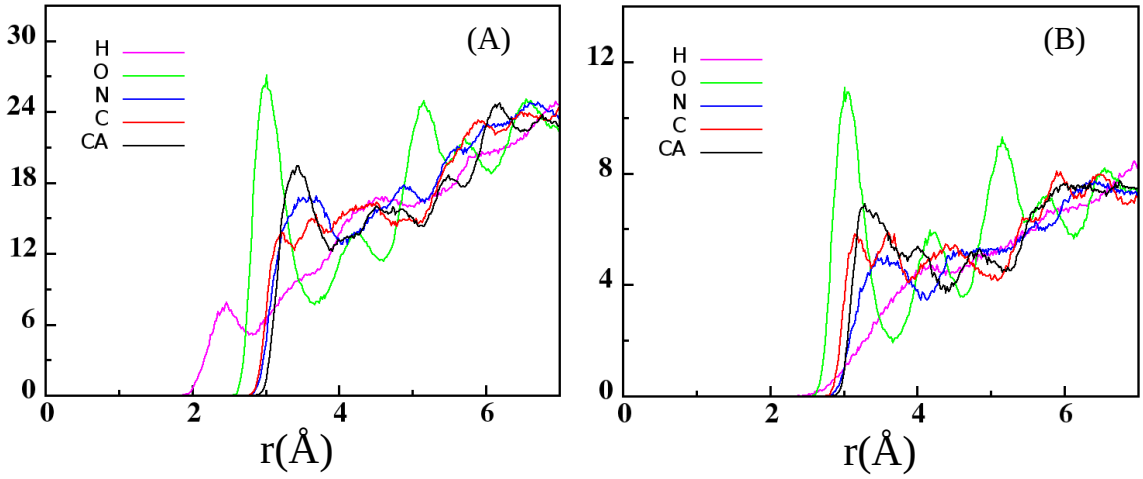

Fig. 2 RDFs for the interactions of main chain atoms (i.e., H, O, N, C, CA) of (A) the CMS, and (B) all of the Gly residues in the CMS with AuNS. The first peaks of RDFs in (A) for all of the main chain atoms at a distance of less than 3.5 Å demonstrate that AuNS directly interacts with the protein backbone. The first peaks of RDFs in (B) for all of the main chain atoms at a distance with a relationship of r(O) < r(C) < r(CA) < r(N) < r(H) further confirms the conformation of Gly residues on AuNS displayed in Fig. 1(B). The peaks of the RDFs for the carbonyl oxygen in both (A) and (B) are sharper and higher compared to those for other main chain atoms.

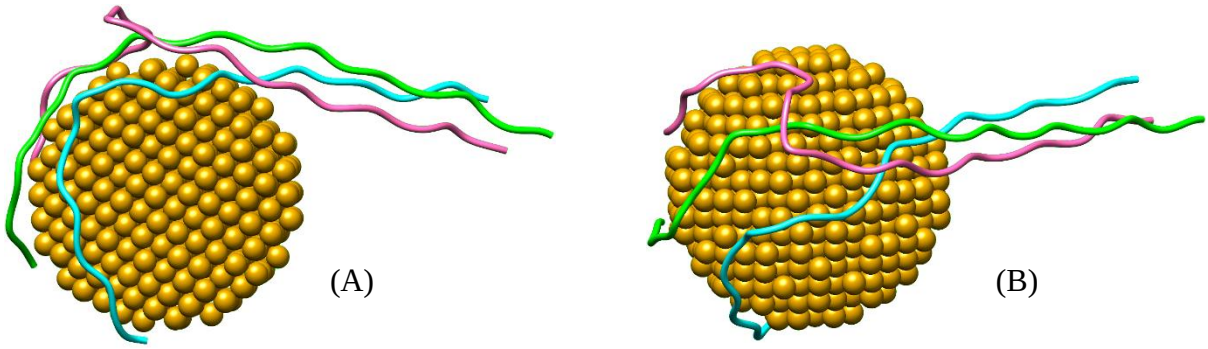

Fig. 3 (A) front view and (B) top view of a representative snapshot of the CMS-AuNP complex, where the CMS is unfolded on the AuNP with a diameter of 3 nm. The CMS only partially interacts with the AuNP with a diameter of 3 nm, but the portion of the CMS adsorbed on the AuNP unfolded severely.

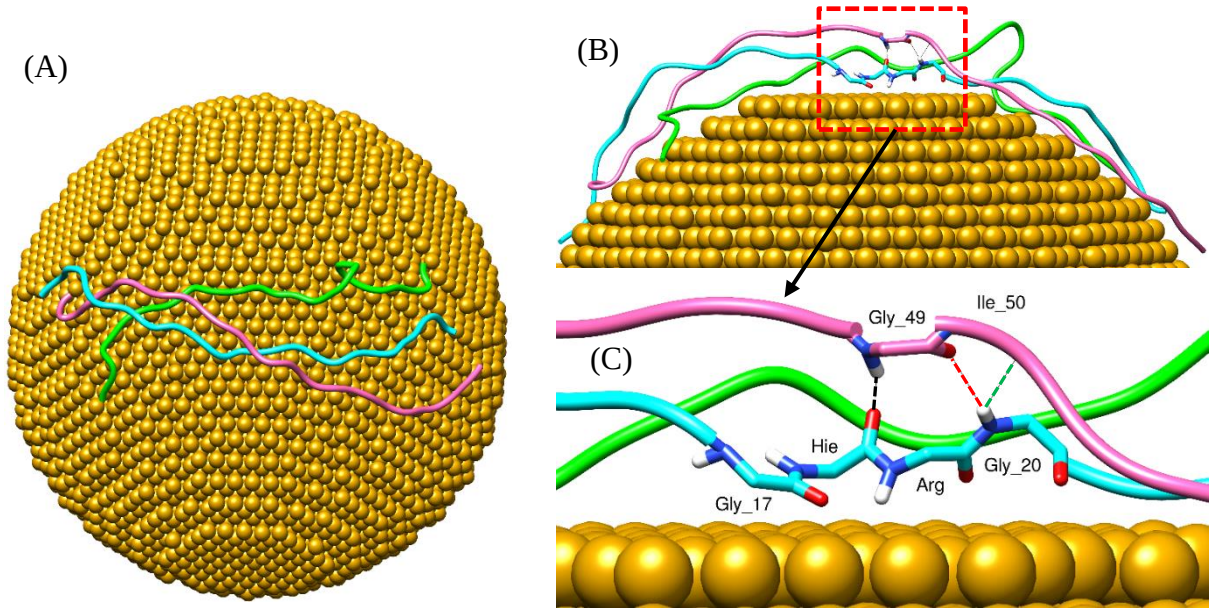

Fig. 4 (A) top view and (B) front view of a representative snapshot of the CMS-AuNP complex, where the CMS is unfolded on the AuNP with a diameter of 8 nm. The CMS fully adsorbed on the AuNP with a diameter of 8 nm, and the intact molecule unfolded significantly. (C) is a zoomed in view of the complex within the red dashed rectangular in (B), where the CMS interacts with the Au(1 1 1) facet of the AuNP. For clarity, only the main chain atoms are showed for Gly_17, Hie_18, Arg_19, Gly_20 and Gly_49 residues. Only when an amide hydrogen in one chain and a carbonyl oxygen in a neighboring chain face towards each other (the axis of the triple helix), they may form inter-chain hydrogen bonds as indicated by the dashed lines in (C).

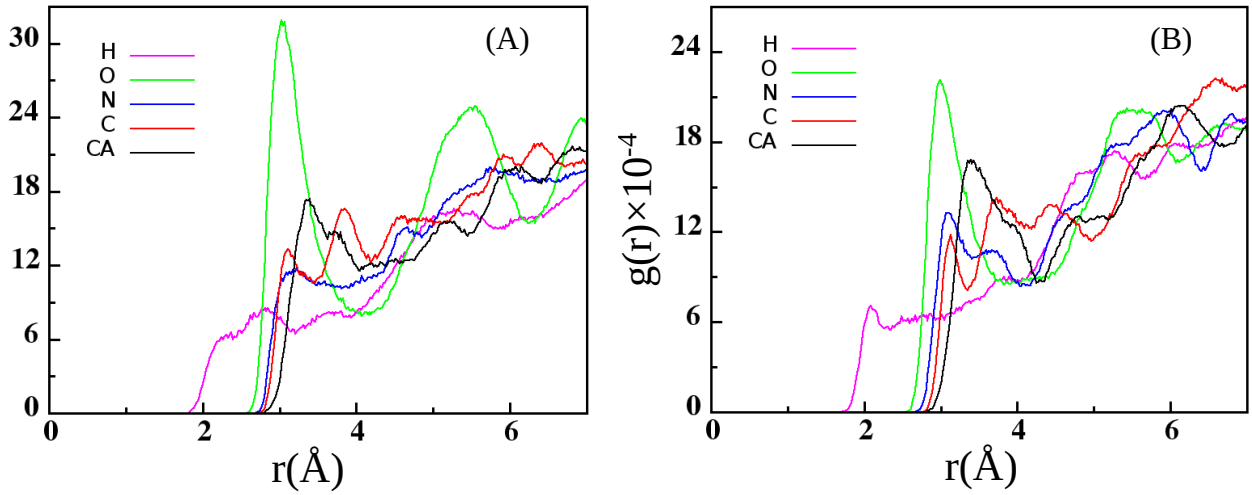

Fig. 5 RDFs for the interactions between the CMS and the AuNP with a diameter of (A) 3nm and (B) 8 nm. The first peaks of RDFs in (A) and (B) for all of the main chain atoms occur at a distance of less than 3.5 Å. The peaks of the RDFs for the carbonyl oxygen in both (A) and (B) are sharper and higher than those for other main chain atoms.

Table 1. Model information of systems of the CMS in the presence and absence of AuNS and AuNPs.

Model information	Sys. 1	Sys. 2	Sys. 3	Sys.4
Water box type	Triclinic	Octahedron	Octahedron	Octahedron
Water box dimension	157 Å × 159 Å × 90 Å	113 Å × 113 Å × 113 Å	105 Å × 105 Å × 105 Å	117 Å × 117 Å × 117 Å
Counter ions (number)	Cl^- (7)	Cl^- (7)	Cl^- (7)	Cl^- (7)
Number of gold atoms	8064	Nil	887	15707
Number of water molecules	68651	33538	26217	26787